INTERNATIONAL UNION OF PURE AND APPLIED CHEMISTRY

MACROMOLECULAR DIVISION

COMMISSION ON POLYMER CHARACTERIZATION AND PROPERTIES

WORKING PARTY ON STRUCTURE AND PROPERTIES OF COMMERCIAL POLYMERS*

A STUDY OF IMPACT STRENGTH TESTING AND ITS RELEVANCE TO REAL MOULDINGS

Prepared for publication by
S. TURNER
Plastics Division, Imperial Chemical Industries Ltd.,
Welwyn Garden City, Herts., UK

A STUDY OF IMPACT STRENGTH TESTING AND ITS RELEVANCE TO REAL MOULDINGS

S Turner

Imperial Chemical Industries Limited, Plastics Division,
Welwyn Garden City, Herts

Abstract - The impact resistance of simple mouldings as assessed by various
impact machines has been compared with that of standard specimens cut from them, as
part of a search for test procedures that will give good correlations with the
resistance of commercial end-products in service.

The falling dart tests appear to be the most versatile of those used in this
programme and are particularly informative when the test conditions are such that
the material under investigation is in, or near to, its tough-brittle transition.

1 INTRODUCTION

The measurement of impact strength is an essential part of any materials evaluation
programme. Most of the test methods are basically simple, but the results which emerge are
far from straightforward, primarily because impact strength is not a single, inherent,
physical property but rather a combination of several. Data on impact strength suffer from
two deficiencies; the first is that there can be wide discrepancies between results for
nominally identical batches and the second is that laboratory results often correlate poorly
with service performance. These deficiencies are attributable in part to the well-known
sensitivity of impact strength to processing variables, but the second one is attributable
also to factors associated with mould and gate geometry in the case of injection mouldings,
to the design of extrusion heads, and to the size of the object under consideration.

The programme discussed in this report, and its sequel now under way, has concentrated on
the second deficiency because it is the more important, albeit the one that has received the
less attention. Various doubts have been expressed over the relevance of data derived from
small, idealized test specimens to the service behaviour of mouldings of complicated shape
and often of large size. In many instances the poor correlations have necessitated the
adoption of tests of the actual end-products which is unsatisfactory in many respects. The
main objective of the experimental programme was to compare results obtained on mouldings
tested as entities, or at least on large pieces of such entities, with those obtained from
the common standard tests on specimens cut from those mouldings. The various participants*
contributed to the programme in accordance with their preferred standard practices and there
was some overlap in the tests carried out in the different laboratories, but the programme
was not designed as a statistical exercise by which interlaboratory variability could be
measured and no attempt is made in this report to derive such information. In fact, the
report contains no serious statistical analysis, because this would have produced several
statistically significant but physically meaningless trends which would serve no purpose
other than to confuse what is inevitably a complex picture. Similarly, for simplicity, many
of the experimental results are omitted.

2 SAMPLE AND TEST DETAILS

The material used in the programme was a commercial propylene homopolymer 'Moplen' T30 S,
supplied by Montedison (Participant F). This material is suitable for both injection
moulding and film extrusion. The Melt Flow Index of the batch was 2.9 (ASTM D1238, L), its

---

* The participants of the working party were:-

BASF (identified as A)		Montedison	(F)
Borg Warner	(B)	Rhone-Poulenc	(G)
Hoechst	(C)	Shell	(H)
ICI	(D)	TNO	(I)
Monsanto	(E)		

intrinsic viscosity was 190 ml/g (tetraline, 135°C), its isotacticity index was was 95–96%
and its polydispersity ratio M_w/M_n was 7.8. The material was moulded by Montedison into
open-topped boxes with a hexagonal base and by Rhone-Poulenc (Participant G) into rectan-
gular plaques. The former, see Fig. 1a, provides corners and other features commonly found
in moulded articles and the latter, see Fig. 1b, provides two types of weld region, an
"opposing flow" weld in Plaque Type 1 and a "merging flow" weld in Plaque Type 2. The walls
and the base of the boxes were approximately 3 mm thick and the plaques were approximately 4
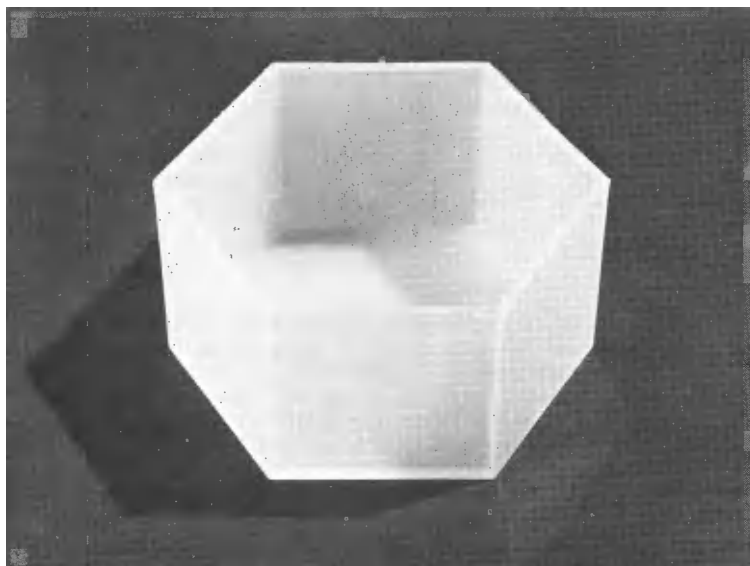mm thick.

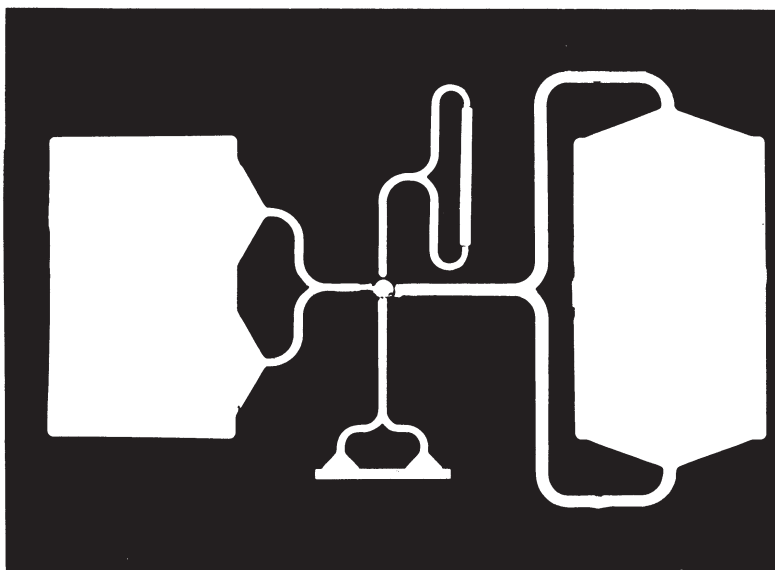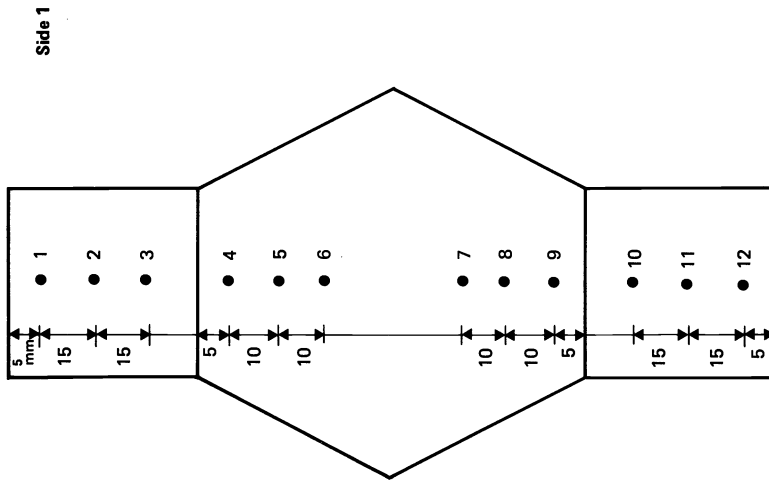Fig. 1a. Boxes. Moulded by Montedison (Participant F).

Fig. 1b. Plaques. Moulded by Rhone-Poulenc (Participant G).

Position	Block Number			
	A9	A19	B9	B19
1	902.7	902.5	902.2	902.0
2	902.9	902.4	902.8	902.2
3	903.4	902.5	902.4	903.1
4	903.8	903.7	903.8	903.2
5	903.4	903.6	903.7	902.9
6	903.6	904.0	904.2	904.1
7	903.9	904.1	903.7	904.6
8	904.4	904.4	904.7	903.7
9	902.4	902.8	902.5	901.9
10	903.2	902.9	903.1	904.0
11	902.5	901.5	901.6	904.0
12	901.5	902.3	901.1	903.0

Figure 2 a: Density Distribution Within and Between Boxes

Densities in kg/m^3

Type I Plaque
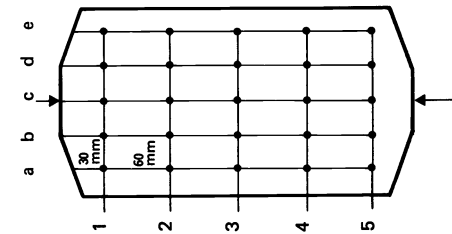
Batch C (No. C 129)

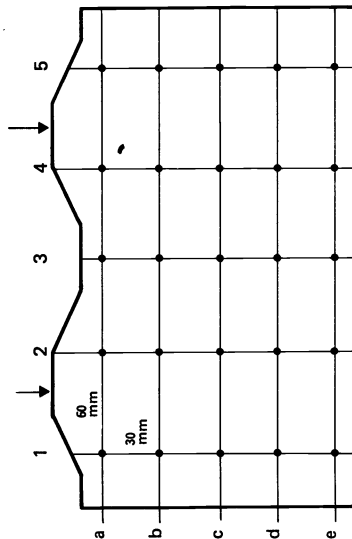| Position	a	b	c	d	e
1	903.5	904.6	904.4	904.6	903.8
2	904.4	904.3	904.9	903.8	904.6
3	904.4	903.5	903.9	903.7	904.6
4	903.2	904.5	903.5	903.8	903.8
5	903.8	904.4	904.2	904.5	904.2

Batch D (No. D 459)

Position	a	b	c	d	e
1	903.9	904.8	904.7	904.1	903.8
2	903.7	904.3	903.3	905.3	905.0
3	904.5	904.5	905.2	903.6	904.6
4	902.8	902.2	903.2	903.6	902.2
5	903.9	905.1	905.0	904.1	904.3

Type II Plaque

Batch C (No. C 129)

Position	1	2	3	4	5
a	903.8	904.3	904.4	904.3	902.3
b	904.2	904.0	904.2	903.9	904.5
c	904.0	903.9	905.0	904.0	905.0
d	904.2	903.3	904.4	903.9	903.9
e	903.6	903.9	903.4	903.9	902.2

Batch D (No. D 459)

Position	1	2	3	4	5
a	904.4	904.2	904.0	904.1	903.8
b	905.1	904.8	904.4	904.4	904.6
c	905.6	904.2	903.5	903.7	903.8
d	904.9	905.1	904.4	904.4	905.0
e	903.9	903.7	904.1	904.1	904.3

Figure 2b: Density Distribution Within and Between Plaques
Densities in kg/m³

The boxes were moulded by means of a reciprocating screw machine with a screw diameter of 45 mm and a L/D ratio of 15.2. Four different sets of moulding conditions were used during exploratory trials in an attempt to define "good" and "bad" processing conditions. There were no significant differences in the impact strengths and a choice was made, therefore, on the basis of other properties. The conditions under which two batches, designated A and B, were moulded are listed in Appendix 1. The mouldings were numbered sequentially and grouped into blocks of 25 which were distributed randomly to the various participants. Full details of the distribution have been recorded but are not reported here. Records of the pressure in the hydraulic circuit and of the axial displacement of the screw were obtained for the 15th and 25th moulding in each block, in case the experimental results revealed any inter-block variability but it transpired that any such variability was overwhelmed by other factors.

The moulding conditions for the plaques were not deliberately chosen to give good and bad batches but inadvertent changes during the production run were such that the mouldings were separated into two batches designated C & D, with potentially different impact character-istics. As with the boxes, these were numbered sequentially, grouped into blocks and allocated to the participants in a random manner.

Participant F measured densities on some of the boxes and some of the plaques, using a density gradient column in accordance with ASTM D1505. The positions of the specimens and the results are given in Figs. 2a and 2b. There was a significant range of density within the boxes (approximately 3 kg/m^3), the maximum density in any box occurred in the base and the density variation was not symmetrically disposed in relation to the sprue. No one who is familiar with the injection moulding process will be surprised by such results but, on the other hand, no one concerned with testing can ignore such variations. The variation within the plaques was similar to, though slightly smaller than, that within the boxes, and the "average" density of the plaques was slightly higher than that of the boxes though the difference was smaller than the variations within each moulding.

The densities of the boxes were measured about six months after they were moulded. The elapsed time for the plaques was about four and a half months. If the storage time of the plaques had been equal to that of the boxes a slightly larger difference between the average densities might have emerged but the programme was planned in the knowledge that the changes in impact strength that are known to occur after an article has been moulded become progres-sively less marked as time passes, so that although true equilibrium is never reached, an approximation to it is attained after about 3 months. Figure 3, in which notched Charpy impact data have been plotted against storage time, suggests that the changes became insignificant after about 30 days, though the scatter on impact data is such that slight trends are difficult to detect.
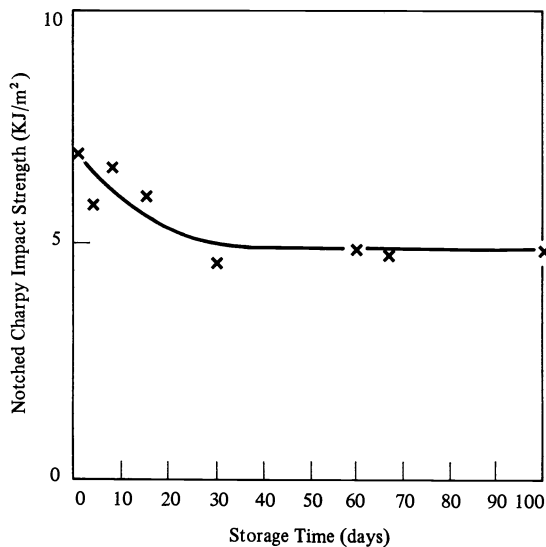

Fig. 3. The effect of ageing on impact strength.

The various tests were therefore scheduled to be carried out not less than three months and not later than five months after the moulding operations and the specimens were to be stored at 23°C and 50% RH. There were minor infringements of the limits on the storage time by some participants but none was such as to invalidate the results or introduce a discrepancy attributable to storage effects.

The impact resistance was measured by several different methods, some standard, some slightly different from standard and others unique to particular laboratories. The contributions of each participant and brief details of the test methods are given in Appendix 2, and at appropriate points in the main text. Except in one experiment, which is discussed in Section 4.1, the tests were all carried out at 23°C.

In the following discussion of the results the plaques are considered first, partly because the experimental results are more concise and partly because the moulding is inherently simpler, apart from the weld line which is a feature that can be isolated for study.

3 IMPACT PROPERTIES OF THE PLAQUES

3.1 General Features (Plaques)

Impact strength is so sensitive to molecular orientation, crystallinity and crystal texture that some variations in the strength from point to point are to be expected in injection mouldings. This is particularly true of regions of flow discontinuities such as weld lines, etc, though it transpired that the weld region in the plaques was not much weaker than areas remote from the weld except in one specific type of test. The mouldings were slightly anisotropic and judgements on possible small differences between Batches C and D could be correspondingly uncertain but most of the experiments were so arranged that any significant differences would be discerned and the overwhelming evidence is that the batches were virtually identical in impact resistance.

The simplest statement on the similarity of the batches is by Participant A who used a hydraulically actuated tensile tester at cross-head speeds of 0.05 m/s and 5 m/s on specimens conforming to the recommendation of ASTM D1822S. Several specimens were taken from each of two plaques to produce the results given in Table 1.

TABLE 1. High-speed tensile properties, Participant A.

Batch and Plaque Number	Crosshead Speed (m/s)	Yield Stress (MN/m^2)	Coeff. of Variation (%)	Rupture Stress (MN/m^2)	Coeff. of Variation (%)	Elongation at rupture (mm)	Coeff. of Variation (%)
C151	0.05*	44.0	5.8	35.8	11.3	1.95	15.7
	5+	–	–	62.9	4.9	1.31	8.4
D381	0.05*	45.1	3.0	38.2	6.8	1.93	8.3
	5+	–	–	62.1	6.4	1.61	6.6

* Mean Values from 5 specimens.
+ Mean Values from 20 specimens.

These results show no significant differences between the two plaques and hence, by inference, between Batch C and Batch D.

Participant H measured yield stress at a much slower rate (0.0008 m/s) obtaining an average value of 34.6 MN/m^2 for Type 1 plaques and 34.2 MN/m^2 for Type 2 plaques. There was again no significant variation from point to point in the plaques, though the mean values for specimens cut in such a way as to incorporate the weld were in all cases marginally lower than those cut so as not to incorporate it. The impact results obtained by the same participant using specimens taken from the same positions in the plaques give no hint of a weakness in the weld in the Type 1 plaque but some suggestion of one in the Type 2 plaque. However, no clear conclusion about this can be drawn from these results because anisotropy arising from molecular orientation is an alternative explanation. No distinction was made between Batches C and D in this set of tests.

The data, which are based on six specimens, are given in Table 2. It incorporates a footnote diagram giving code-letters for the positions of specimens within each plaque; this cutting plan was recommended by the moulders, Participant G, and although it was not followed scrupulously by the other participants it nevertheless constitutes a convenient reference grid.

TABLE 2. Impact data and yield stress for plaques.
Batches C and D used indiscriminately. Participant H.

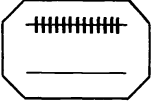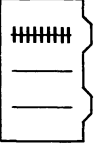| Plaque Type	Position Code	Yield Stress[+] (MN/m^2)	Unnotched Charpy Impact Strength[x] (kJ/m^2)	Notched Charpy Impact Strength[x] (kJ/m^2)	Izod[□] Impact Strength (kJ/m^2)	Tensile[°] Impact Strength (kJ/m)
	a	34.6±0.4	93± 6	2.8±0.1	2.1±0.3	130±15
	b		94±10	2.8±0.1	2.5±0.1	
	c	34.2±0.3	78±11	2.8±0.1	2.1±0.4	128±10
1	d		65±18	2.9±0.3	1.9±0.2	
	e	34.7±0.3	96± 8	2.8±0.1	1.8±0.3	165±30
	f	34.9±0.2	88±19	2.8±0.1	1.7±0.5	155±10
	g	34.1±0.3	99±15	1.3±0.5	1.5±0.0	165±10
	h		108±14	1.5±0.1	1.5±0.1	
2	i	34.0±0.3	108±13	1.6±0.2	1.6±0.2	180±10
	j		62± 9	1.4±0.1	1.4±0.1	
	k	34.4±0.1	128±14	1.7±0.1	1.8±0.1	210±10
	l	34.4±0.2	125± 5	1.6±0.3	1.6±0.3	225± 5

Position key, Type 1 Plaque

Position key, Type 2 Plaque

[x] ASTM D 256 B
[□] ASTM D 256 A
[°] DIN 53448
[+] ASTM D 638 IV

These results indicate that unnotched specimens from Type 2 plaques were tougher than those from Type 1 plaques and that the reverse is true for the notched tests. This could have arisen from different levels of molecular orientation in the two plaques and in at least partial support of this tentative explanation there is clear evidence in Table 2 of aniso- tropy in the Type 2 plaques commensurate with the general orientations to be expected from the positions of the gates. The data for the Type 1 plaque are much more ambiguous in that specimens from positions e and f had higher tensile impact energies than the others, despite their transverse orientation with respect to the main flow direction; however, the head-on merging of the melt fronts would tend to disrupt the simple flow patterns and lead to irregularities in the molecular orientation. A weakness at the weld could also contribute to the anomaly.

Tensile impact data obtained by Participant D give a clearer indication of the anisotropy. Specimens were cut with their major axis parallel to, or perpendicular to, the flow direction, distributed along rows as indicated in Table 3. Thus the results are mean values

TABLE 3. Tensile impact-plaques. Non-standard specimens. Participant D.

Plaque Type	Specimen Location Axis Direction	Position Code (Row Number)		Batch C Mean Value $(\bar{x})$ (kJ/m^2)	Batch C Standard Deviation (s) (kJ/m^2)	Batch D Mean Value $(\bar{x})$ (kJ/m^2)	Batch D Standard Deviation (s) (kJ/m^2)
1	Specimen axis parallel to flow direction		1	67	5	60	7
			2	54	6	63	8
			3	66	8	67	6
	Specimen axis perpendicular to flow direction		4	54	13	60	7
			6	65	10	57	5
2	Specimen axis perpendicular to flow direction		1	51	12	58	7
			2	57	9	63	2
			3	57	7	54	7
	Specimen axis parallel to flow direction		4	58	10	62	5
			6	68	8	65	7

within particular plaques, in contrast with the mean values in Table 2 which were derived from several plaques for specific positions. The apparent discrepancy between the numerical values in the two tables arises merely from the different specimen geometries, that used by Participant D being non-standard. (See Appendix 2).

These data show no significant differences between Batches C and D. The same is true of all the other experiments on plaque and therefore, in the interests of brevity and clarity, the data for the two batches are merged in this report rather than being set out in full detail as evidence of the similarity. The two types of plaque have similar strengths and both are anisotropic. Overall, there is no consistent evidence of weakness at the weld, which would appear in Table 3 as lower values for Row 2 than for Rows 1 and 3. However, the failures were ductile under the chosen test conditions (tensile impact and Charpy) but the use of notched specimens and/or faster straining rates could take the conditions sufficiently close to the tough-brittle transition for clearer distinctions to emerge. This is discussed in later sections.

3.2 Impact Energies from Standard Tests (Plaques)

Participant B carried out notched Charpy impact tests in accordance with DIN 53453 using a cutting plan closely similar to that shown below Table 2, the difference being that specimens a and b were replaced by a single specimen, denoted a/b, and c and d were replaced by c/d. The specimens were 50 mm x 6 mm x 4 mm with 2.7 mm of material behind the notch; they were tested on a Zwick impact tester and the initial speed of impact was 2.9 m/s. Mean values based on five specimens are plotted in a bar chart in Fig. 4a for which it is clear that the notched Charpy impact strength of specimens cut from the plaques was independent of the type of plaque, the position of the specimen in relation to the plaque and the position of the notch in relation to the weld, ie there is no evidence of weakness at the weld.

Izod impact strengths measured by the same participant in accordance with ASTM D 256 at an impact speed of 3.46 m/s were independent of position in the plaque and similar for both batches. The data in Fig. 4b suggest that the Type 2 plaque was stronger than the other, whereas the evidence from Participant H (Table 2) indicates the reverse and that from Participant F (Table 4) indicates that the two types of plaque had similar strengths. The comparison in Fig. 4b is not entirely satisfactory because the specimens from the Type 2 plaque were cut out by a circular saw whereas those from the Type 1 plaque were milled. The observed order of merit is the reverse of what might have been expected though the predominant factor would be the quality of the notch, variations in which may account for the different conclusions that can be drawn from the three sets of data.
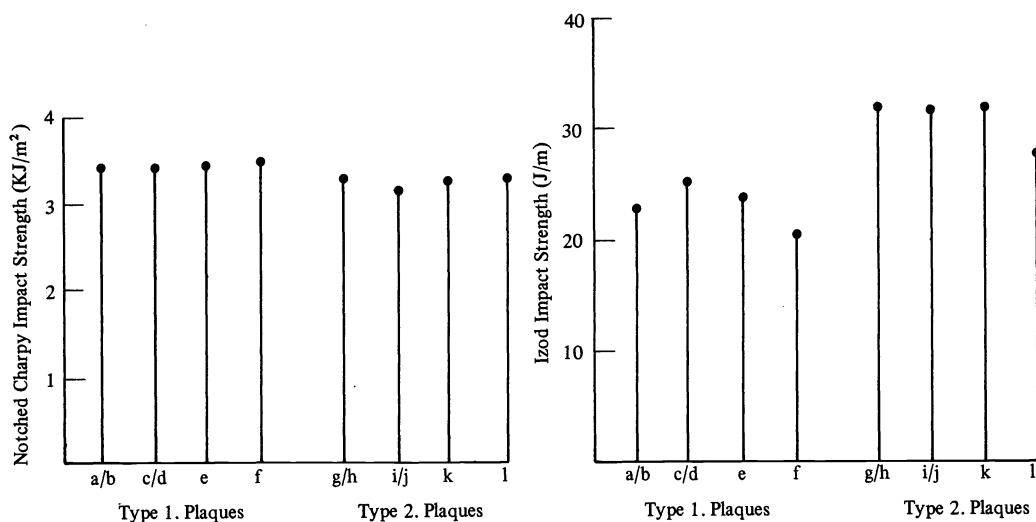

Fig. 4. (a) Notched Charpy impact strength (mean values from 10 specimens).
        (b) Notched Izod impact strength (mean values from 5 specimens).

TABLE 4. Izod impact strength (kJ/m^2). Participant F.

Plaque Type	Axis Direction	Position Code (Row Number)	$\overline{x}$	s	n
1	Specimen Axis Parallel To Flow Direction	1	1.9	0.2	16
		3	2.1	0.2	16
		1 + 3	2.0	0.2	32
	Specimen Axis Perpendicular To Flow Direction	5*	1.6	0.2	31
2	Specimen Axis Perpendicular To Flow Direction	1	1.8	0.2	16
		3	1.8	0.1	16
		1 + 3	1.8	0.2	32
	Specimen Axis Parallel To Flow Direction	5*	2.0	0.2	32

* Row Number 5 is mid-way between Rows 4 and 6, see Table 3.

On balance, it is reasonable to conclude that the two types of plaque yield notched Izod specimens with virtually identical strengths and that they exhibit a low degree of aniso-tropy that is consistent with the flow paths (Participant B's data, in Fig. 4b, give no indication of anisotropy).

3.3 Crack Growth in Very Sharply Notched Specimens (Plaques)

Very sharply notched specimens were tested by three of the participants who, between them, used a wide range of specimen geometries. Although these experiments were a crucial part of the main study, they can also be regarded as a self-contained subsidiary study of the value of a fracture mechanics analysis as a means of merging the results from various tests into an overall picture of properties or performance. The experimental results exhibit a wide variability and certain illogical features which, at first sight, tend to dispel such hopes of unification but which are attributable merely to the material and some of the test geometries violating the conditions under which linear elastic fracture mechanics can be applied legitimately. In Participant B's tests, specimens corresponding to the positions a/b, c/d, e and f (see previous section and Table 2) were notched to various depths midway along one edge and stretched at about 0.08 mm/s. The critical stress-field intensity factor as calculated from equation 2.1 (Appendix 2) is plotted against a/W, the ratio of notch depth to specimen width, in Fig. 5. Its marked sensitivity to a/W and the whitening of the specimens near the notch indicate that the calculated values are spurious.

Despite this unwanted sensitivity of apparent K_{IC} to a/W, inspection of the datum points at any approximately constant value of a/W shows that there was no weakness at the weld and no anisotropy in the resistance to crack propagation in Type 2 plaques. The data for Type 1 plaques are very similar though they cannot be interpreted quite so unambiguously because in these plaques weakness at the weld would have been at least partly offset by any anisotropy. The approximate bounds of the data for Type 1 plaques are marked in Fig. 5 by short horizon-tal lines.
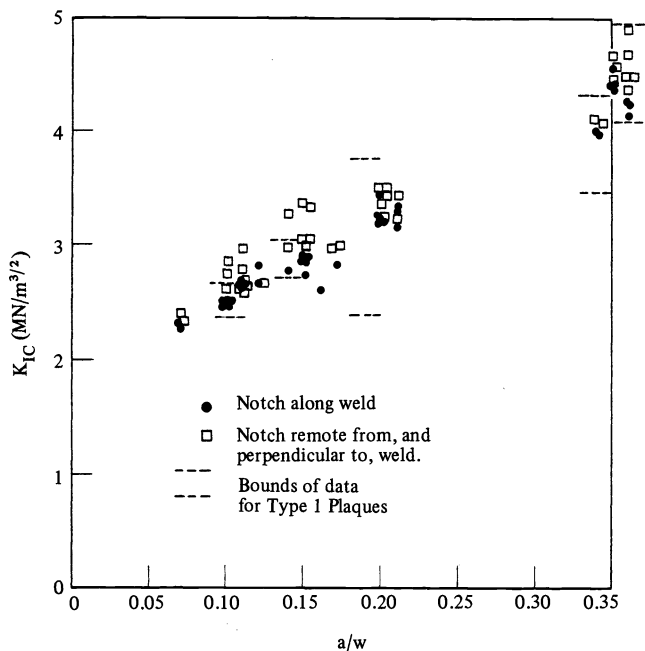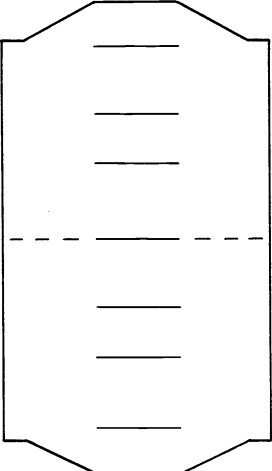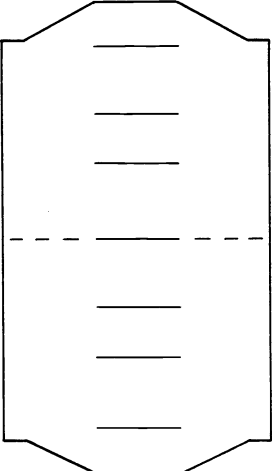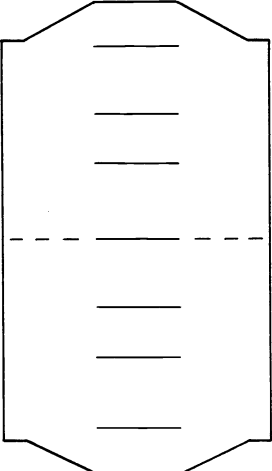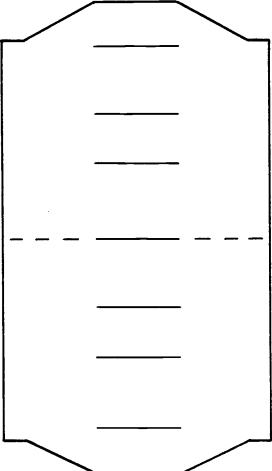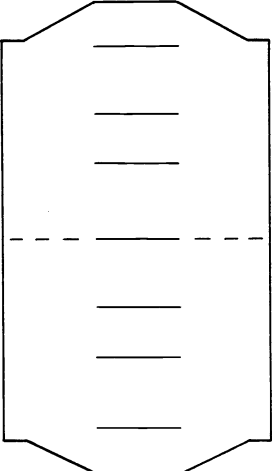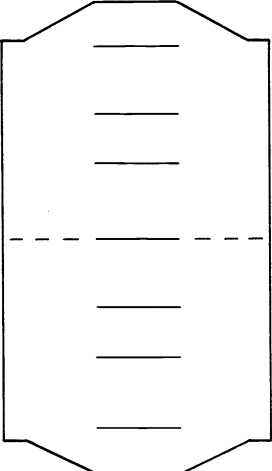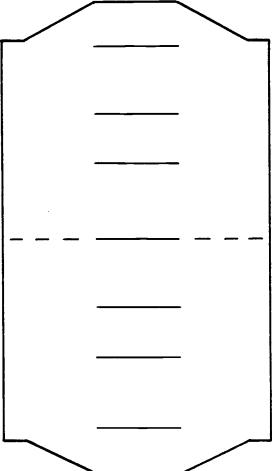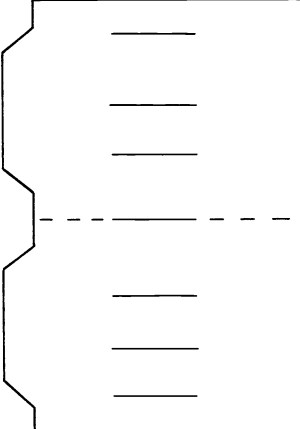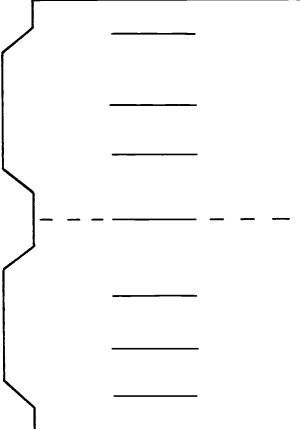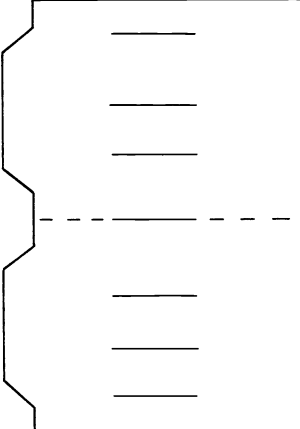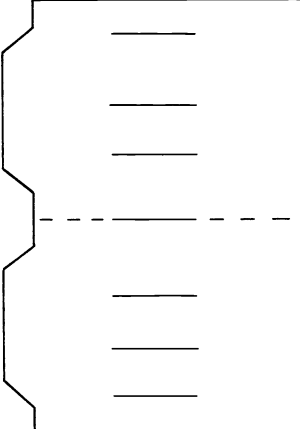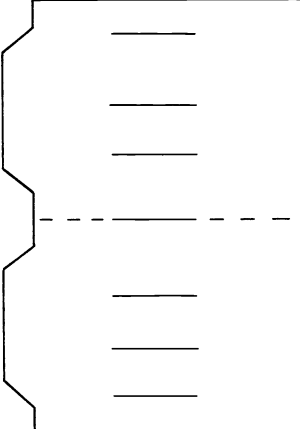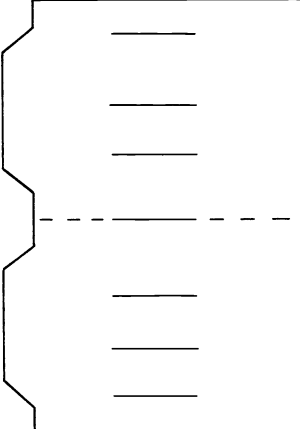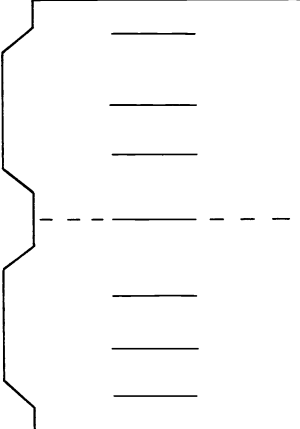

Fig. 5. Effect of a/W ratio on apparent K_{IC} from single-edge-notched specimens cut from Type 2 plaques.

Participant D used rectangular plates approximately 150 mm x 130 mm with either a central notch about 38 mm long or two edge notches each about 22 mm long; the plates were tested in tension at a cross-head speed of approximately 0.17 mm/s. All the specimens failed in an apparently brittle manner. The mean value of K_{IC} from all the tests on Type 1 plaques was 4.1 $MN/m^{3/2}$, with standard deviation of 0.5 $MN/m^{3/2}$. The corresponding result for the Type 2 plaques was 3.9.

TABLE 5. K_{IC} centre-notched plates. Participant D.

Plaque Type	Specimen Identification	K_{IC} (MN/m$^{3/2}$)
1	1	4.3, 4.5
	2	4.7, 4.0
	3	4.5, 4.9
	4	(3.8, 4.0, (3.5, 4.0,
	5	4.6, 4.1
	6	(3.6, 4.8, (4.1, 4.1
	7	4.7, 4.2
2	1	4.8, 4.3
	2	(3.8, 3.8, (4.2, 4.1
	3	4.2, 4.1
	4	(4.0, 3.6, (4.1, 4.2
	5	4.3, 4.1
	6	3.7, 3.8
	7	3.5, 4.7

Tests on plates notched at different distances from the weld gave no clear evidence of weakness near the weld, see Table 5, but the results were very scattered. Subsidiary experiments, on which two plates were cut from each of several consecutively numbered Type 1 plaques, confirmed that the scatter could be ascribed to inter-plaque variability and/or variability in the notching process.

One of each pair of plates had a notch parallel to the injection direction and one had a notch perpendicular to it, and the results given in Table 6 indicate that the resistance to crack propagation parallel to the main flow direction was lower than that perpendicular to it, in agreement with the conclusions to be drawn from the other tests (eg Tables 3, 4), though the significance of the fracture mechanics data is not quite at the 5% level.

TABLE 6. Reproducibility of results from sharp-crack tests on Type 1 Plaques.
K_{CI} (MN/m$^{3/2}$) from plates with a central notch.

Plaque Number	K_{IC}, notch parallel to flow direction	K_{IC}, notch perpendicular to flow direction
23	4.3	4.1
24	3.8	4.1
25	3.7	3.7
26	3.6	5.5
27	3.5	4.6
28	3.8	4.2
$\bar{x}$	3.8	4.4
s	0.3	0.6

The third participant measured K_{IC} by means of sharply-notched Charpy and micro-Charpy specimens. Data for Type 1 plaques, in Table 7, show some anisotropy in the resistance to crack propagation and a significant difference between the values derived from the two

TABLE 7. K_{IC} (MN/m$^{3/2}$). Micro-Charpy and Charpy specimens.
Type 1 plaques. Participant F.

Test Method	Notch Direction	$\bar{x}$	s	n
Micro-Charpy	Perpendicular to flow direction	1.98	0.06	55
	Parallel to flow direction	1.84	0.07	43
Charpy	Perpendicular to flow direction	2.64	0.26	57
	Parallel to flow direction	2.34	0.25	62

test geometries. The micro-Charpy specimens would have been subjected to a higher straining rate than the Charpy specimens and hence one might assume that the former give the better approximation to the true value of K_{IC}. This conclusion is supported by other results from the same participant. Micro-Charpy specimens with various notch depths gave calculated K_{IC} and G_{IC} values that were virtually independent of notch depth as a/W ranged from 0.1 to 0.5, see Fig. 6. These specimens were cut from Type 1 plaques with the notch lying perpendicular to the flow direction. The mean value of 1.8 MN/m$^{3/2}$ is slightly lower than that given in Table 7, whereas one might have expected it to be higher if anything because the span of the test specimens was greater (48 mm instead of 36 mm). However, it is possible that the specimens had changed during the period between the acquisition of the data in Table 7 and of those in Fig. 6. It is recognised that the ageing effect is generally slight after the first few days, (see Fig. 3 for example), but a progressive reduction in fracture toughness accords with the other known facts (1) and therefore the slight apparent inconsistency between the data in Table 7 and those in Fig. 6 may be regarded as trivial.
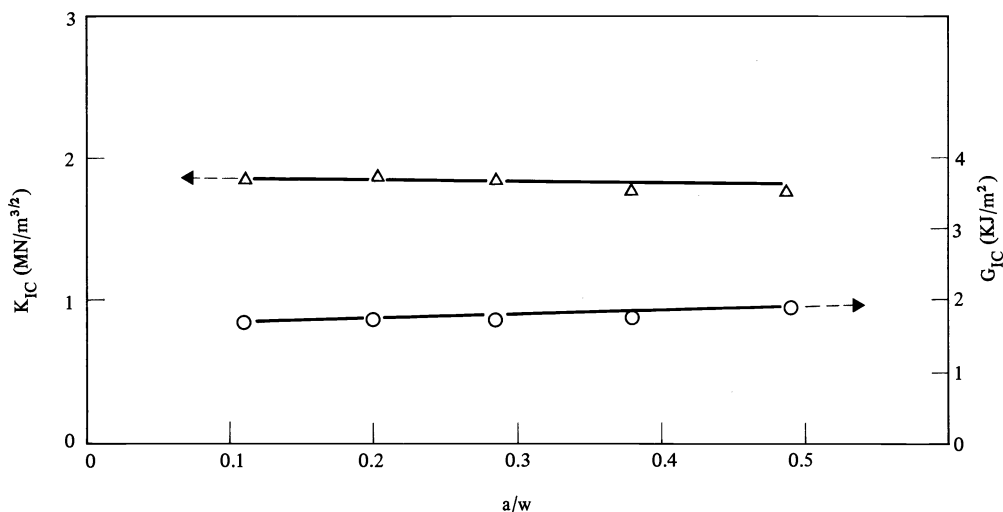
Fig. 6. K_{IC} and G_{IC} as functions of a/W. Micro-Charpy specimens cut
          from Type I plaques with notch perpendicular to main flow direction.
          Participant F.

It seems reasonable to assume that the plane strain value of K_{IC} is approximately 1.8
$MN/m^{3/2}$. The various higher values derived from the other tests are spurious because of
violations of the stringent constraints that must apply in any fracture mechanics test on an
inherently tough plastic. Even though the plate tests all gave seemingly brittle fractures
and values of K_{IC} in good agreement with the results obtained from independent experiments
by the same participants on other mouldings made from a different polypropylene (2), the
high values of 3.5– 4 $MN/m^{3/2}$ may not be a true measure of K_{IC}, though it can be argued
that they are evidence of a significant rate-dependence of the plane-strain fracture
toughness.

3.4   Falling Dart and Driven Dart Impact Energies (Plaques)
This group of tests is always regarded as being in a different class from the other standard
tests, as indeed it is in some important respects, and in this set of experiments it has
turned out to be more discriminating than the others.

In Participant D's experiments approximately square plates were freely supported on a steel
ring of inner diameter 50 mm, and struck by a steel ball 12 mm in diameter at a speed of 5
m/s. The input energy was approximately 150J so that the impactor was decelerated only
slightly during any of the tests. Six plates were cut from each plaque. They were so
placed in the test machine that the face marked by the ejector pins was in compression
during the impact, though the marks themselves were well away from the point of impact. In
Table 8 the individual results are given since they illustrate so emphatically the enormous
range of the impact energies, the large variations within any one plaque and a marked
weakness in the plates encompassing the weld line. The mean values and the standard
deviations are summarized in Table 9. The lower strength associated with the weld line is
either significant or highly significant (99% confidence) for both types of plaque. It
emerges also that plate number 2 was significantly weaker than plate number 5 in Type 2
plaques.

Participant F tested clamped discs at an impact speed of 4.4 m/s and an input energy of 60J.
A correction was applied to the measured impact energy in those cases where it was a
significant proportion of the input energy. The dart diameter was 20 mm and the inner
diameter of the support ring was 60 mm. The weld was a source of weakness in these experi-
ments also, though the effect was less marked than it is in Tables 8 and 9. In Participant
F's experiments some specimens were tested with the ejector-pin marks on the tension face of
the disc and some with the marks on the compression face. The specimens were positioned so
that the marks coincided with the region of maximum stress during the tests. Those plates
with the ejector-pin marks in tension during the test were much weaker than those with the
marks in compression, see Table 10. Type 1 plaques behaved similarly. Weakness at the weld
was less clearly demonstrated by this group of tests but this is largely because the effect
of the ejector-pin marks was so dominant.

TABLE 8. Falling dart impact energy (J). Participant D.

Plaque Type	Plaque Number		Absorbed Energy (J)					
1	23 303		1* −	3.4	2 1.7	1.5	3 12.9	10.1
	24 304		4.9	3.6	3.2	1.1	15.6	7.0
	233 523		2.7	6.3	0.9	1.0	10.2	6.1
	234 524		4.0	3.4	1.0	0.7	4.8	7.4
	23 303		4 4.0	9.1	5 1.9	2.6	6 14.2	2.7
	24 304		5.9	4.9	10.3	2.3	3.3	14.6
	233 523		4.8	10.3	2.8	1.1	20.9	8.9
	234 524		2.0	11.6	3.3	0.7	8.8	12.2
2	23 303		1 10.1	14.8	2 2.0	2.8	3 5.5	6.3
	24 304		7.4	8.4	2.4	2.8	9.0	6.8
	233 523		3.9	5.7	4.5	4.3	4.0	9.9
	234 524		4.8	7.1	3.3	11.0	6.2	3.4
	23 303		4 23.3	16.4	5 5.0	7.4	6 10.8	9.8
	24 304		7.3	20.2	2.2	7.0	11.1	12.9
	233 523		14.0	17.8	3.3	8.9	12.4	30.4
	234 524		21.8	17.1	8.1	11.2	5.1	17.3

* Plate identification numbers

TABLE 9. Falling dart impact energy (J) near to and remote from weld line. Participant D.

Plaque Type	Plate Identification	$\bar{x}$	s	n
1	Remote from weld 1,3,4 & 6*	7.8	4.6	31
	Near weld 2,5	2.3	2.3	16
2	1,3,4,6	11.3	6.5	32
	2,5	5.4	3.1	16

* See Table 8 for position key.

TABLE 10. Falling dart impact energies (J). Type 2 plaques.
The effect of ejector-pin marks. Participant F.

Plate Identification	Stress-field at ejector-pin marks	$\bar{x}$	s	n
1 Weld excluded	Tension	0.6	0.2	8
	Compression	10.3	5.3	10
2 Weld included	Tension	1.7	0.5	10
	Compression	6.4	3.0	10
3 Weld excluded	Tension	1.3	0.4	10
	Compression	10.2	5.7	10

Participant E used both a conventional falling dart and a "driven dart" (3). Four plates approximately 106 mm x 76 mm in size were cut from each plaque, two of the four encompassing the weld region. In the falling dart test the diameter of the impactor was 31.75 mm, the diameter of the clamp ring was 57.15 mm and the speed of impact was initially 3.60 m/s. In the driven dart test the diameter of the impactor was 25.4 mm, that of the support ring was 57.15 mm and the speed of impact was 2.54 m/s. The results, which relate to Type 1 plaques only, are summarized in Table 11 with the identities of the batches preserved. The falling dart test failed to detect any weakness at the weld in contrast to Participant D's test (Table 9). However the driven dart did so, and also an apparent superiority of Batch D over Batch C.

TABLE 11. Comparison of falling dart and driven dart impact energies (J).
Type 2 plaques. Participant E.

Test Method	Batch	Impact on weld line		Impact away from weld line	
		$\bar{x}$	s	$\bar{x}$	s
Driven Dart	C	4	4	36	34
	D	35	38	78	35
Falling Dart	C	26		31	
	D	32		29	

The one conclusion that emerges clearly from the falling dart and driven dart experiments is that the weld lines were weaker than unwelded areas under conditions of high speed impact with high input energy. The combination of polymer grade, moulding conditions, specimen geometry and impact speed was such that the specimens were close to their ductile-brittle transition at the test temperature, and irregularities such as a weld-line or a mark on the tension face were sometimes sufficient to change the nature of the failure by causing a crossing of the transition. Figure 7 shows the failure energy vs probability of failure in the driven dart test and the bimodal distribution typical of a mixture of brittle and ductile failures is clearly apparent.
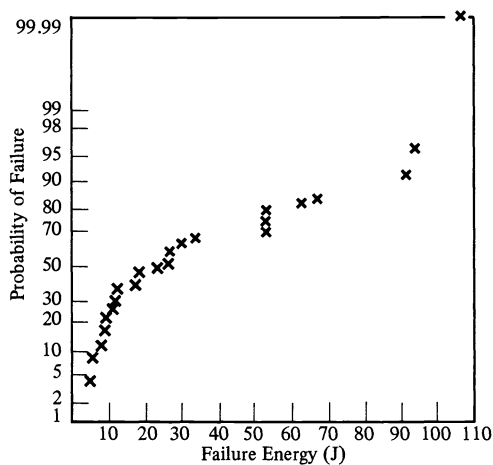
Fig. 7. Bimodal distribution of failure energies in driven dart test on Type 1 plaques. Point of impact remote from weld line.

4 IMPACT PROPERTIES OF THE BOXES

4.1 General Features (Boxes)

The test programme for the boxes was very similar to that for the plaques, except where the different specimen geometry offered different opportunities. The results are reported and discussed according to a pattern that closely parallels that adopted in the sections devoted to the plaques, but it would have been both tedious and unrewarding for this course to have been followed too slavishly and therefore strict comparability is preserved only where it serves a specific purpose.

Thus, for instance, there is no equivalent to Table 1 for the boxes because the yield stresses and rupture stresses were very similar to those for specimens cut from the plaques. On the other hand, comparisons between the results for specimens cut from the boxes and those cut from the plaques are included wherever it seems appropriate.

The first issue to be resolved for the boxes was whether specimens cut from different sides had different impact resistances. Participant I combined an investigation of this with a determination of the sensitivity of the impact resistance to temperature using the Charpy test in nominal accordance with ISO/R 179-1961. Circular notches were used instead of square ones and the specimens had to be 2.8 mm wide instead of the stipulated 6 mm. The specimens were tested at an impact speed of 2.9 m/s in a commercial Charpy Impact Tester (Zwick Type 5102) fitted with a nitrogen gas thermostat described elsewhere (1).

The specimens were cut from the boxes in a special order to limit the number of tests needed. The locations of the 36 specimens taken from the sides of two boxes for the tests

Fig. 8. Charpy impact strength. Specimens cut from sides of boxes.

at each temperature are shown in Appendix2. Mean values are plotted in Fig. 8, which shows the usual features of impact strength affected by temperature, not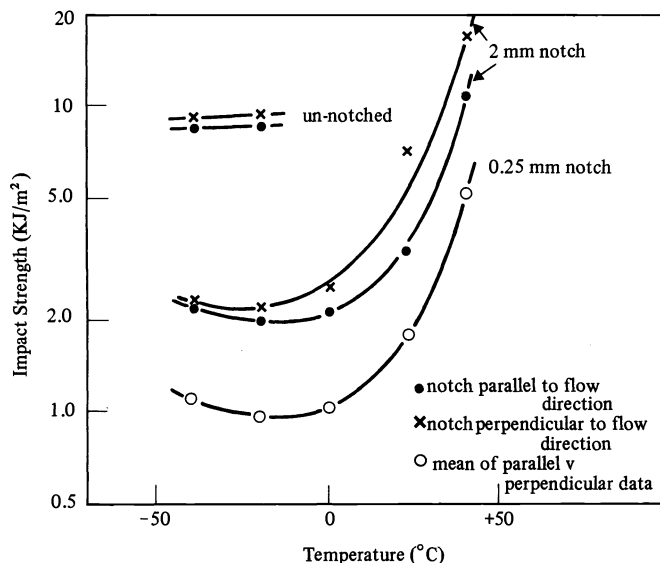ch geometry and molecular orientation. The coefficient of variation of themeasurement is 8% for unnotched samples, 13% for samples with a 2 mm radius notch, and 11% for samples with a 0.25 mm radius notch, which is not large. In general there is no extra variation due to the samples having been taken from different boxes, an exception being the specimens with a 2 mm radius notch. These show an extra variation of 15% mainly due to large deviations in the temperature region associated with steep increase in the impact strength.

The number of specimens used in these tests was so small that any judgement on the possible differences between the six sides would be highly dubious without recourse to some strategem. Accordingly, logarithmic means have been taken over all temperatures for each notch geometry and each side, from which it is reasonable to conclude that there were no significant differences between the sides, even though the density distribution discussed in Section 2 would lead one to expect otherwise. The results are set out in Table 12.

TABLE 12. Logarithmic mean values of Charpy impact strength (kJ/M^2) over all temperatures. Batch A. Participant I.

| Notch Geometry | Side Identification | | | | | | | Coefficient of variation of mean (%) | |
	1	2	3	4	5	6	Mean	observed	calculated
Unnotched	8.8	8.8	9.6	8.3	8.7	9.0	8.9	5	4
Notch radius 2mm	3.8	3.8	3.7	3.7	3.5	3.8	3.7	4	4
Notch radius 0.25 mm	1.6	1.6	1.5	1.7	1.6	1.6	1.6	4	4
Weighted total mean	3.0	3.1	3.0	3.0	2.9	3.0	3.0	2	2

* Calculated value when there is only a measurement variation.

In the last two columns of this table the coefficient of variation arising in the tests on the six sides is compared with the coefficient for each notch geometry calculated from the mean values. For six measurements the difference between the highest and lowest value can be about four times the standard deviation. Since the observed differences are smaller, the observed variation coefficient can only contain a small contribution from the variation coefficient between the sides, ω. An estimate of the highest value of ω can be obtained from the confidence limit for the distribution of variance ratios, v^2, given by ref 4.

$$1 + n \frac{\omega^2}{\sigma^2} < v_{0.95}(f_\sigma, f_\omega) \times \frac{s_2^2}{s_1^2} \qquad \ldots\ldots (1)$$

where n = number of measurements (in total 24)
     f = number of degrees of freedom (for σ, f = 55; for v, f = 5)
     S_1 = variation coefficient due to the measurement variation
     S_2 = variation coefficient found between different sides

From this relationship, with σ = 11%, and a confidence limit of 95%, it follows that ω is at most 4%. It can be concluded that the differences between the six sides of the box were negligible. Further analysis indicates that the impact strength was not affected by the position within each side but that it did depend on the orientation of the specimen with respect to the flow direction, except in the case of specimens with a notch tip radius of 0.25 mm.

The conclusions reached in the previous paragraph arose from a detailed analysis of a relatively small number of results and it is comforting for the experimentalist to have corroborative results from tensile impact tests carried out by Participant D. The mean values given in Table 13 show no evidence of differences between the sides other than what can be attributed to anisotropy. There is evidence that the boxes moulded from Batch A were

less anisotropic than those from Batch B; specimens from the latter with their axis paral-
lel to the flow direction absorbed a significantly greater energy than corresponding speci-
mens from Batch A, and the reverse was true for the transverse specimens. Although the
comparison for the transverse specimens is not statistically significant (probably because
of the peculiarly large standard deviation for the Batch A data), it seems reasonable to
attribute any difference between Batches A and B to different molecular alignments reflec-
ting the relative ease of moulding.

TABLE 13. Tensile impact. Specimens from sides of boxes.
Participant D.

Batch	Specimen Orientation	Side Identification	Mean Value[+] (kJ/m^2)	Standard Deviation (kJ/m^2)
	Specimen axis parallel to flow direction	2	71.1	5.5
		4	73.0	5.4
A		6	69.2	8.5
	Specimen axis perpendicular to flow direction	1	67.5	17.0
		3	65.9	10.6
		5	66.7	17.1
	Specimen axis parallel to flow direction	2	75.0	5.1
		4	75.5	6.4
B		6	76.1	8.5
	Specimen axis perpendicular to flow direction	1	65.0	5.3
		3	62.5	6.3
		5	63.1	3.9

[+] Twelve specimens in each case, three taken from each of four boxes
    (No's 7, 13, 14, 18). No distinction made for position in the side.

An overall summary of the anisotropy in the plaque or the boxes for all four batches is
presented in Table 14, the positions of the specimens and the type of plaque having been
ignored.

TABLE 14. Tensile impact energy (kJ/m^2). Participant D.

Type of Moulding	Specimen Orientation	Batch	$\bar{x}$
	Specimen axis parallel to flow direction	A	71.1
		B	75.5
Box	Specimen axis perpendicular to flow direction	A	66.7
		B	63.5
	Specimen axis parallel to flow direction	C	62.7
		D	63.6
Plaque	Specimen axis perpendicular to flow direction	C	55.9
		D	58.6

In a sense the results merely confirm what has already been said about the anisotropy and about the similarity of Batches A and B on the one hand and Batches C and D on the other, but it also emerges that specimens from the boxes had significantly higher tensile impact energies than specimens from the plaques.

Reference has been made in Section 3.1 to the very marked influence that specimen geometry has on tensile impact strength. Comparisons between sets of tensile impact data have to be made with caution for that reason, but that in Table 14 is valid because the specimen geometry was constant in all the tests, except that the specimens from the boxes had slightly shorter ends than the others, because of the dimensions of the box, which only affected the length of the clamped part. Furthermore, firm confirmation of the anisotropy comes from Participant H. Disregarding the positions from which specimens were taken, the mean values (from 48 test specimens) for tensile impact energy measured by ASTM D 1822§ were 68.6 kJ/m^2 for specimens with their axis parallel to the flow direction and 57.2 kJ/m^2 for specimens with their axis perpendicular to the flow direction, using boxes in Batch A. The corresponding values from boxes in Batch B were 69.6 kJ/m^2 and 60.4 kJ/m^2, so there was no discernible difference between Batches A and B. No comparison is possible with the same participant's data for specimens cut from plaques, see Table 2, because different specimen geometries were used for the two series.

4.2 Impact Energies from Standard Tests (Boxes)

It was shown in Section 3.2 that standard notched impact tests were no more sensitive in discriminating between Batches C and D and between Type 1 and Type 2 plaques than the unnotched tests were. There seems little point, therefore, in pursuing the same course in any detailed way for specimens cut from the boxes and instead we will merely compare the data derived from the boxes with the corresponding data derived from the plaques, exploring the difference that apparently emerged from the tensile impact tests of Participant D. It is also apparent, from the results in Section 4.1, that there were no significant differences between specimens cut from different sides of the boxes. A rough check of the data for other notched specimens leads to the same conclusion and therefore for the analysis in this section the specimens from the various sides have all been lumped into a single population.

Participant F's Izod data for specimens cut from boxes are in close agreement with those in Table 4 for specimens cut from the plaques. The latter have a greater spread but if the results for both types of plaque are merged the mean value for specimens with their axis parallel to the flow direction is 2.0 kJ/m^2 (compared with 1.9 kJ/m^2 for corresponding specimens from the boxes) and that for the transverse specimens is 1.7 kJ/m^2 (compared with 1.8 kJ/m^2). However, no such simple picture emerges if Participant H's results are included. These show large differences between specimens taken from the two types of plaque and no close agreement between the specimens cut from plaques and those cut from boxes. The latter, for instance, are also significantly different from the corresponding data obtained by Participant F, see Table 15. Such comparisons underline the difficulties and uncertainties that attend any quantitative assessment of impact resistance; the two participants used the same test method on specimens cut from nominally identical mouldings and yet produced results differing by approximately 20%. A temperature difference of 5°C (see Fig. 8) would account for the disparity but that is an unlikely explanation and the real cause was probably small discrepancies in the specimen dimensions or blemishes on the machined surface of the notch.

TABLE 15. Izod impact strength (kJ/m^2). Specimens cut from boxes. Results from two laboratories.

Participant	Specimen axis parallel to flow direction		Specimen axis perpendicular to flow direction	
	$\bar{x}$	s	$\bar{x}$	s
F	1.9	0.2	1.8	0.3
H	1.6		1.5	

The good agreement between specimens cut from boxes and specimens cut romplaques in Participant F's experiments is not a priori irreconcilable with the poor agreement in Participant H's experiments, because in the latter some of the specimens from the plaques were taken from the region of the weld whereas in the former such specimens were excluded. However if the weld was a source of weakness, which was far from obvious in all but the most severe tests, Participant H's plaque data should have indicated a lower impact energy than the box data did, whereas the reverse was observed.

It could be argued, after inspection of Table 2, that the trends in Participant H's Izod data are supported by the notched Charpy data, but a comprehensive consideration of Charpy results which takes the results of other participants into account shed confusion rather than clarity on the issue. Mean values derived from tests carried out in accordance with three different specifications, but with no participant using more than one method, are set out in Table 16. The experimental coverage was not sufficient for hard comparisons to be made but there is obviously a fairly high variability between results from different specifications and, in the one case where a direct comparison is possible, there was poor agreement between two laboratories using a common specification. However, despite the variability, it can be inferred that specimens from the boxes had a lower notched impact strength than those from the plaques, which is the reverse of what might have been expected from the difference in thickness of the two sources of specimens.

TABLE 16. Notched Charpy impact strength (kJ/m^2). Specimens taken from boxes and plaques.

Partici-pant	Test Method	Specimen axis parallel to flow direction			Specimen axis perpendicular to flow direction		
		Box	Type 1 Plaque	Type 2 Plaque	Box	Type 1 Plaque	Type 2 Plaque
B	DIN 53453		3.4	3.3		3.5	3.3
D	Internal Standard similar to ASTMD 256	1.9			1.7		
E	DIN 53453		2.7	2.8		2.7	2.7
G		2.2			2.3		
H	ASTMD 256B		2.8	2.8		1.7	1.5
I	Modified version of ISO/R 179-1961	1.8			1.8		

4.3   Crack Growth in Very Sharply Notched Specimens (Boxes)

Participant D used four sharp-notch geometries, double-edge-notched (DEN) specimens about 10 mm wide, large double-edge-notched specimens consisting of entire sides of the boxes, the hexagonal bases with a central notch approximately 20 mm long and complete boxes with the same sized notch. The specimens were all tested in tension at a crosshead speed of about 0.8 mm/s. Participant F tested very sharply notched micro-Charpy specimens in flexure at an impact speed of 2 m/s. More details are given in Appendix 2.

The small DEN specimens fractured by slow crack growth so that the critical stress field intensity factor was not derived. Analysis of the results shows that there were no systematic differences between specimens cut from different sides of the boxes, no anisotropy and no difference between the two batches. The mean value of the stress field intensity factor at crack initiation, K_I, based on 64 results, was 1.81 $MN/m^{3/2}$ with a

standard deviation of 0.03 MN/m$^{3/2}$. The other specimen geometries used by Participant D all produced failures that were brittle, at least under superficial examination. The mean values of the apparent K_{IC}, for notches parallel to the flow direction and with the data for the two batches merged, were 4.4 MN/m$^{3/2}$ for double-edge-notched sides, 3.8 MN/m$^{3/2}$ for centrally-notched bases and 3.7 MN/m$^{3/2}$ for complete boxes with a central notch in the base. This trend in the value of K_{IC} reflects the effects of specimen size and degree of constraint.

The micro-Charpy data obtained by Participant F gave the much lower value of 1.79 MN/m$^{3/2}$ for the stress field intensity factor which is not very different from the value for specimens cut from the plaques (1.92 MN/m$^{3/2}$ from Table 7). The close correspondence of these values and also of the data for the plates implies that the plaques and boxes constitute very similar test samples on the basis of resistance to crack propagation. The standard notched Izod data led to the same conclusion but the standard notched Charpy data suggest that the plaques and the boxes constitute different samples.

4.4 Falling Dart and Driven Dart Impact Energies (Boxes)

Participant D used the same excess-energy falling dart test for the boxes as for plates cut from the plaques, with such changes in the support system as were necessary to conform to the recommendations of Participant F, the moulders, with whom the various configurations are standard test practice. The details of these test configurations are given in Appendix 2. Many boxes from each block were committed to these tests. For instance, eight bases and six complete boxes from each of four blocks were used, half being tested with the face containing the sprue mark in tension and half with it in compression. Within the limits set by a relatively large experimental scatter, there was no discernible difference between the blocks or between the two batches. The results for the various blocks and the two batches have been combined in Table 17 to show the highly significant effect of the sprue scar for both the bases and the complete boxes.

TABLE 17. Falling dart impact energy (J). Participant D.

Test Configuration	$\bar{x}$	s	n
Base only. Sprue-mark in tension face.	0.30	0.12	29
Base only. Sprue-mark in compression face.	0.64	0.25	32
Complete box. Sprue-mark in tension face.	0.33	0.14	24
Complete box. Sprue-mark in compression face.	1.00	0.35	24

It is evident also that even in the favourable case, ie. where the stress field at the sprue scar was compression, the failure energy was generally much less than that for plates cut from the plaques (see results in Tables 4, 5 and 6) even when ejector pin marks and weld lines exerted complementary weakening effects. Only some of the difference can be attributed to the plaques being thicker than the boxes, and the deficiency is almost certainly due to the diverging flow regime that would have existed near the sprue during the moulding operation and to the residual strains that are a characteristic of the region in fabricated articles.

The same participant also used test configurations F6 and F7. The edges common to neighbouring sides were weak, as would be expected, but the energies absorbed, between 1.5J and 2J, were significantly higher than those reported in Table 17 because the high flexibility allowed relatively large movements of the point of impact. On the other hand the maximum force developed during such tests was lower than those arising during the tests on bases and complete boxes. This group of results have little quantitative merit and they are not discussed further.

Participant F's results follow a similar pattern, the details of which are not given here though it is pertinent to note that a distinction could be made between the energy to produce the first signs of damage and the total energy for complete failure whereas no such distinction could be drawn in Participant D's results. The "first damage energy" of the former corresponds fairly closely to the entire failure energy of the latter, whereas the total failure energy of the former is roughly four times as large. This difference between the two sets of results is attributable to the many (mainly minor) differences between the two apparatus and test procedures, but particularly to the differences in impactor velocity and input energy.

Participant C used a third method, following DIN 53443. The specimens were clamped hydraulically over a circular support with an inner diameter of 40 mm, and struck at an impact velocity of 4.43 m/s by a dart with a hemispherical head 20 mm in diameter. The input energy was 186J. The specimens were mounted in such a way that the erstwhile outside surface of the box was in tension during the impact test. Mean values for test on sides and bases, in each case based on between seven and ten results, are given in Table 18.

TABLE 18. Falling dart impact energies for the first signs of damage (J). Participant C.

Batch and Block Identity	Part Tested	$\overline{x}$	s	n
A17	Side No 1	1.1	0.6	10
	Base	0.4	0.4	8
B17	Side No 1	10.9	13.6	10
	Base	0.3	0.1	10

As with most of the other falling dart results, the standard deviations are high but despite this it is clear that the box sides from the B17 sample were definitely tougher than those from the A17 sample, on the basis of the proportion of high energy failures in the test population. The sides were tougher than the bases, presumably because of the deleterious effects of the sprue scars though there may have been a contributory factor associated with a marked difference between the observed birefringence in the skin layers of the side and that of the base. There were no major differences in the birefringences of Batch A and Batch B.

The overall conclusions to be drawn from the falling dart tests on boxes are that the bases and the complete boxes were brittle under the prevailing conditions. The sides were less brittle and some could be described as tough; with absorbed energies greater than 30J. The radial orientation in the centre-gated bases, the flow irregularities associated with the sprue region and the scar left by removal of the sprue were all detrimental to the strength and they combined to reduce the impact energies to levels lower than those recorded in the tests on plates cut from the plaques.

5 CONCLUDING COMMENTS

The third line of the Introduction to this report stated that the results which emerge from impact tests are "far from straightforward" and most of the tables in the subsequent text bear that out. With hindsight it has become clear that the possible differences between Batches A and B on the one hand and Batches C and D on the other were insignificant; thus, that aspect of the programme need not have been so exhaustive. Statistically significant differences were found, but in some cases results from different tests were in direct conflict and we have to conclude that unsuspected extraneous factors were operating during some of the experiments, to confer an apparent statistical significance that had no underlying physical significance. On the other hand, the splitting of each set of mouldings into two distinct batches with potentially different impact resistances was the decision of experienced technologists who judged the fluctuation in moulding conditions to have been sufficient to warrant such a step, and the fact that the impact resistances turned out to be virtually identical may perhaps be taken as indicating that the moulds had been so well designed that only extremely unfavourable processing conditions could have produced weak mouldings. In general the various tests detected the anisotropy in the mouldings, but this was at a relatively low level which is a further tribute to the mould design and which also suggests that an extension of the programme might explore the effect of bad processing conditions.

Only the falling dart and the driven dart tests detected weakness at or near the weld. The results from this group of tests were also sensitive to flaws such as marks from the ejector pin cavities and the scar arising from the removal of the sprue. This superior discriminating power of the dart tests is in one sense merely a matter of chance, arising simply because the critical features of this group of tests combined to put these particular specimens near to their tough-brittle transition during the impact. Because of this proximity, the effect of additional influences such as stress concentrators in the tension face or weld lines could change what would otherwise have been a ductile failure into a brittle one. A change of processing conditions, such as those that delineated the batches, could cause a similar shift through the transition and there is some evidence of this in Tables 11 and 18.

The distribution of the failure energies in the falling dart test was usually either obviously bimodal or implicitly so. This is evidence of the proximity of the tough-brittle transition under the conditions prevailing during the test. In contrast, except for very occasional manifestly freakish results, the other tests produced ductile failures if the specimens were unnotched and brittle or nominally brittle failures if the specimens were notched. At some lower temperature the unnotched specimens would be brittle, at some higher temperature the notched specimens would be tough and at certain intermediate temperatures the distributions of failure energies for such specimens might be bimodal. A more exhaustive study of the strength of the welds in the plaques using temperature and notch geometry as the independent variables, ie. an extension of Participant I's experiments, might provide more fundamental information than was forthcoming from the falling dart tests, and might allow the weakening effect of the weld to be equated to aspecific stress concentration factor or at least to a specific notch geometry. The Charpy specimen would be suitable for that purpose, though presumably the other test specimens would be similarly discriminating along the temperature axis.

If the various test methods give essentially similar measures of toughness when temperature is used as the primary independent variable, the choice of the most suitable technique for the assessment of the practical impact performance of materials partly reduces to a matter of convenience. However, the impact resistance of a material cannot be isolated from the context of a fabrication process and that is why dart tests tend to be favoured by many of those concened with service performance because entire mouldings or parts of mouldings can be tested directly, and many practical issues, such as the effect of particular flow geometries on end-product performance, can be resolved by appropriate choice of test piece. The value of this type of test is greatly enhanced if the force-deflection relationship, or at least the force-time relationship, is recorded, and due note is taken of the appearance of the damaged specimen. The main disadvantage of the dart method is that the magnitude of the measured energy depends strongly on the shape and size of the part and the stress geometry during impact. This is true for both brittle and ductile failures though it is especially so of the latter. Thus the method is comparative rather than absolute and the results cannot be applied in any general way to engineering design calculations. The other impact tests suffer from the same deficiency, but to a smaller degree, so that they can be regarded as slightly more quantitative. However, the specimens for this group tend to be idealizations bearing little resemblance to practical components so that, with the possible exception of data for very sharply notched specimens, the results are of no greater generality than those from the dart tests. In these circumstances it is likely that, in the future, the dart tests will be used increasingly in preference to the others and, in view of the marked geometry effects, it would be beneficial to all the parties involved if a standard procedure could be defined. It would also be useful if a series of standard test shapes such as the box used in this programme could be adopted universally. These shapes would be identical to, or at least based on, the various mouldings currently used by many companies for in-house testing.

This step towards pragmatism would be in no sense a rejection of sharply notched specimens and fracture mechanics analysis. The results from the latter procedures may relate more to the material than to the structure moulded from it and thereby supplement the falling dart tests usefully, though it is clear that the experiments can be misleading in the absence of indicators as to how closely the measured values of the stress field intensity factor approximate to the plane strain value.

ACKNOWLEDGEMENTS

REFERENCES

1. L.C.E. Struik, "Physical Ageing in Amorphous Polymers and other Materials" Elsevier (1978). Page 196.
2. K.V. Gotham and I.N. Scrutton, Polymer 19, 341-347 (1978).
3. V.A. Matonis, "The Driven Dart Impact Tester for Plastics". Monsanto Co Publication.
4. A. Hald, "Statistical Theory with Engineering Applications", Wiley, N York (1952). Page 381.
5. P.C. Paris and G.C. Sih, "Stress Analysis of Cracks". ASTM Special Technical Publication No 381.
6   W.F. Brown Jnr., J.E. Srawley, "Plane Strain Crack Toughness Testing of High Strength Metallic Materials". ASTM Special Technical Publication No 410.

APPENDIX 1

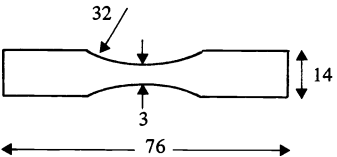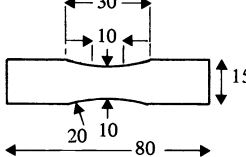MOULDING CONDITIONS
Boxes (moulded by Participant F)

Processing Variable	Batch A	Batch B
Barrel 1 temp., (^{o}C)	181	236
Barrel 2 temp., (^{o}C)	203	247
Barrel 3 temp., (^{o}C)	205	251
Nozzle temp., (^{o}C)	211	208
Moulded temp., neg/pos (^{o}C)	18/30	34/31
Screw (r p m)	85	85
Cooling time (s)	26	26
Overall cycle time (s)	46	51

APPENDIX 2

PROGRAMME AND TEST DETAILS - Principal contributions.

Participant		Test Methods					
		Charpy	Tensile Impact	Izod Impact	Very Sharply Notched Specimens	Falling and Driven Dart	Miscellaneous
A	BASF						High Speed Tensile Tests ASTM D1822S
B	Borg Warner	DIN 53453		ASTM D256	Single-edge-notched specimens in tension		
C	Hoechst					Falling Dart DIN 53443	
D	ICI	Internal Standard Similar to ASTMD 256	Internal Standard		Double-edge-notched strips and plates, centrally notched plates in tension	Internal standard	
E	Monsanto					Internal standard	
F	Montedison	DIN 53453		ASTM D256	Very sharply notched Charpy and micro-Charpy specimens	Internal standard	
G	Rhone-Poulenc						Density
H	Shell	ASTM 256B	DIN 53448	ASTM D256A			Tensile tests ASTM D6381V
I	TNO	ISO/R 179-1961					

SPECIMENS FOR STANDARD TESTS
Tensile impact

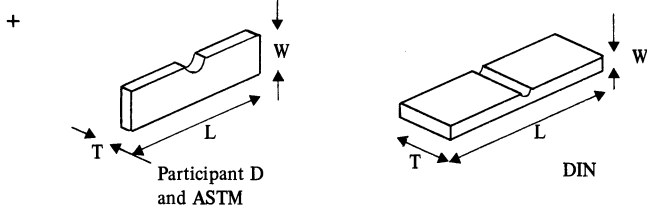|	Participant D	DIN 53448
Impact Velocity (m/s)	2.93	2.9
Jaw Separation ie. Tested Length (mm)	45	45
Specimen Geometry		

Izod

|	ASTM D256-72a
Distance from point of contact of tup to centre of notch (mm)	22
Direction of impact	Parallel to face
Impact velocity (m/s)	3.35
Width (mm)	12.7
Thickness (mm)	12.7
Length (mm)	63.5
Notch	45°V
Notch depth (mm)	Method A,C .25 mm radius Method D 1 mm radius Method E Reversed notch
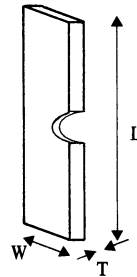
Charpy

| | Participant D | DIN 53453 & ISO/R179-1961E | | ASTM D256-72a |
		Standard Bar	Small Standard Bar	
Type of Loading	4-point	3-point	3-point	3-point
Span (mm)	38.1*	70	40	101.6*
Direction of Impact	Parallel to face (Normal to face when unnotched)	Normal to face	Normal to face	Parallel to face
Impact Velocity (m/s)	2.45	2.9	2.9	3.35
Width (mm)+	6	10	4	12.7
Thickness (mm)+	3	15	6	12.7
Length (mm)	50	120	50	63.5
Notch	45°V 0.25,1,2 mm radius and unnotched	2 mm and unnotched	0.8 mm and unnotched	45°V 0.25 mm radius
Notch Depth (mm)	2.8	3.3	1.3	2.54

* original specification in Imperial units.

+

Participant D and ASTM

DIN

Cutting plan for Charpy tests at low temperatures. Participant I.

⌒ notch, radius 0·25 mm

⬛ notch, radius 2·00 mm
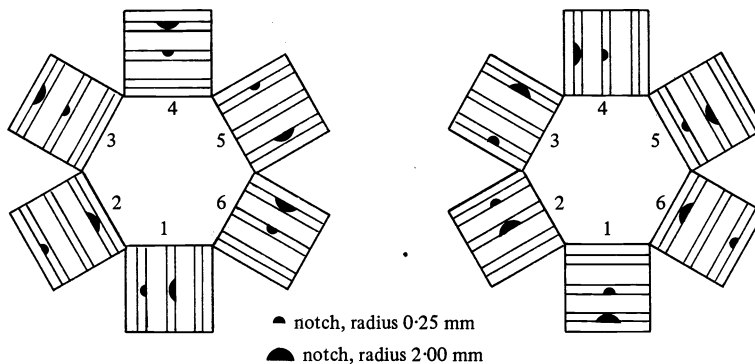
The specimens for the tests at any one temperature were all cut from two boxes.

Falling Dart and Driven Dart

	Participant C (DIN 53443)	Participant D	Participant E		Participant F
			Falling Dart	Driven Dart*	
Inner diameter of support ring (mm)	40	50	57.15	57.15	60
Edge constraint	Clamped	Free	Clamped	Clamped	Clamped
Diameter of impactor head (mm)	20	12	31.75	25.4	20
Impact speed (m/s)	4.43	5	3.60	2.54	4.4
Input energy (J)	186	150	-	-	60

*See ref 3.

Test configurations for dart tests on boxes

F1 — Test of base — F2

F3 — Test of the whole box — F4

F5 — Test of sides without bottom — F6

F7 — 53 mm — Test of corners — 45 mm — F8

rollers
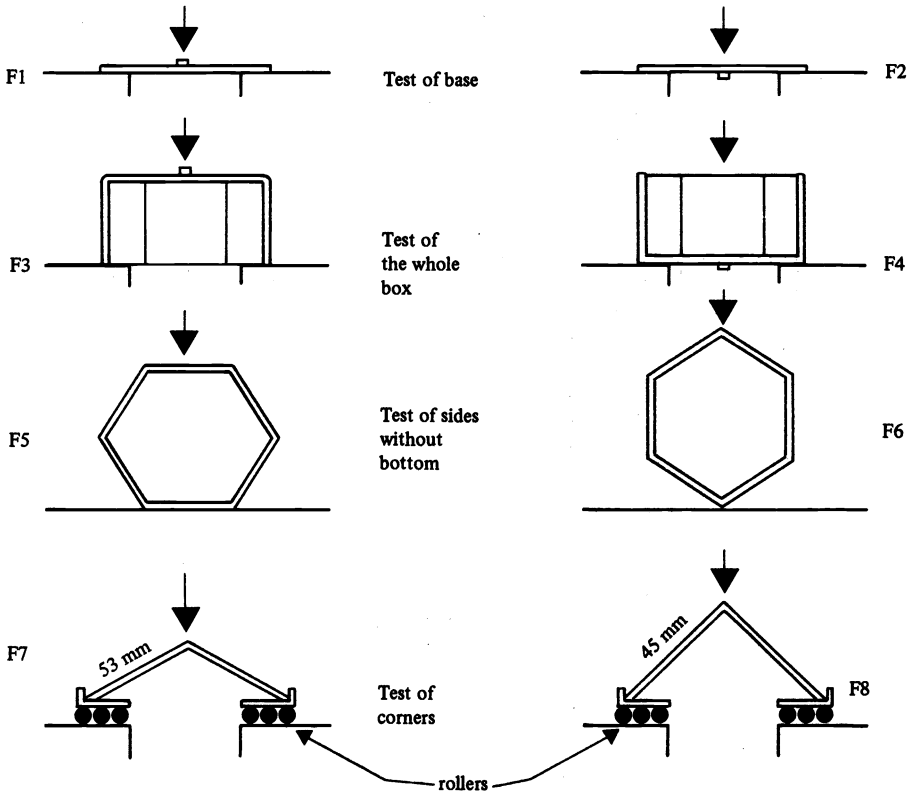
VERY SHARPLY NOTCHED SPECIMENS
Single Edge-Notched Specimens (Participant B).

Length 154 mm, Width 31 mm

Positions in plaques correspond approximately to those shown in
Table 2.

Stress field intensity factor calculated from

$$K_I = \sigma_R \, a^{\frac{1}{2}} \left[1.99 - 0.41 \left\{\frac{a}{W}\right\} + 18.7 \left\{\frac{a}{W}\right\}^2 - 38.48 \left\{\frac{a}{W}\right\}^3 + 53.85 \left\{\frac{a}{W}\right\}^4 \right] \qquad \ldots \ldots \quad (2.1)$$

where σ_R = stress remote from crack
$\quad\quad$ a   = initial crack length
$\quad\quad$ W   = specimen width

Double Edge-Notched Strips and Plates;   Centrally Notched Plates (Participant D).
Stress field intensity factor calculated from:-

$$K_I = \sigma_R (\pi a)^{\frac{1}{2}} \left[\left\{\frac{W}{\pi a}\right\} \tan \left\{\frac{\pi a}{W}\right\} \right]^{\frac{1}{2}} h\left\{\frac{2a}{W}\right\} \qquad \ldots \ldots \quad (2.2)$$

where σ_R = stress remote from crack
$\quad\quad$ a   = initial crack length but measured after fracture
$\quad\quad$ W   = width
$\quad\quad$ $h\left\{\frac{2a}{W}\right\}$ = finite width correction factor which is 1.0 for the
$\quad\quad\quad\quad\quad\quad$ CN specimens (see ref 5 for tabulated values)
$\quad\quad$ K_I = Stress field intensity factor at onset of crack
$\quad\quad\quad\quad\quad\quad$ propagation, based on initial crack length

K_{IC} the critical value of K_I for the onset of unstable crack propagation may
be obtained by the replacement of 'a' in equation 11.2 by a+Δa where Δa is
the length of crack due to slow growth.

Very Sharply Notched Charpy and Micro-Charpy Specimens (Participant F).
$\quad\quad$ Charpy:$\quad\quad\quad\quad\quad\quad$ Specimen$\quad\quad$ 127 mm long, 12.7 mm wide; test span 101.6 mm;
$\quad\quad\quad\quad\quad\quad\quad\quad\quad\quad\quad\quad\quad\quad\quad\quad\quad\quad$ input energy 13.5 J

$\quad\quad$ Micro-Charpy:$\quad\quad\quad$ Specimen$\quad\quad$ 50 mm long, 6 mm wide; test span 36 mm (48 mm
$\quad\quad\quad\quad\quad\quad\quad\quad\quad\quad\quad\quad\quad\quad\quad\quad\quad\quad$ for data in Fig. 6); input energy 4.56 J

$\quad\quad$ Notch depth:$\quad\quad\quad\quad\quad\quad\quad\quad\quad\quad\quad$ Approximately 0.3 of the specimen thickness,
$\quad\quad\quad\quad\quad\quad\quad\quad\quad\quad\quad\quad\quad\quad\quad\quad\quad\quad$ except in special experiments (Fig. 6).

$\quad\quad$ Impact speed:$\quad\quad\quad\quad\quad\quad\quad\quad\quad\quad$ 2 m/s.

Stress field intensiy factor calculated from:-

$$K_I = \frac{3PSa^{\frac{1}{2}}}{2bW^2} Y \qquad \ldots \ldots \quad (2.3)$$

where P = Force to cause fracture
$\quad\quad$ S = Span
$\quad\quad$ b = Specimen width*
$\quad\quad$ W = Specimen thickness*
$\quad\quad$ a = Notch depth
$\quad\quad$ Y = Geometric factor, tabulated in ref 6.

---

* The standard nomenclature on width and thickness is often confusing because W is used to
  represent width in edge-notched tension specimens and thickness in surface-notched flexure
  specimens, in order that a/W has a similar significance in all cases.
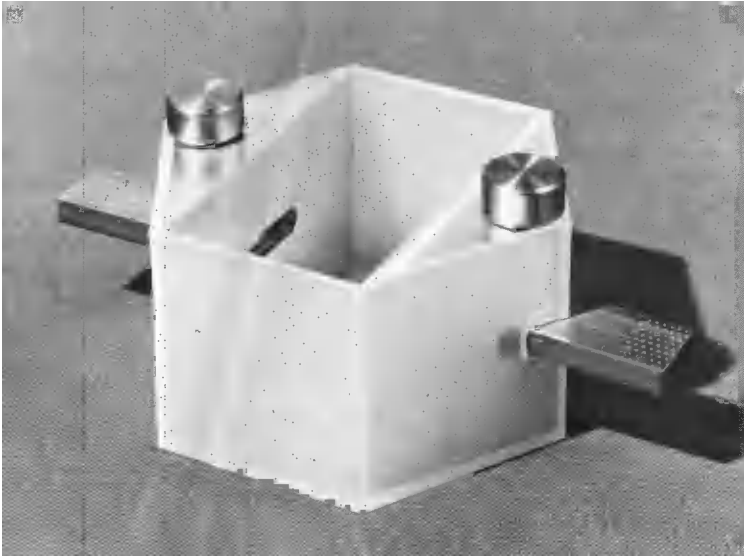
Clamp system for tests on boxes (Participant D).

Tests on Intact Boxes (Participant D)
The system by which complete boxes were tested is shown in the above figure. The inserts
were tapered to match the mould taper so that the force was applied axially to the hexagon.